

1 Marine Cyanobacteria Tune Energy Transfer Efficiency in their Light-harvesting Antennae by 2 Modifying Pigment Coupling

3

4 Authors:

5 Yuval Kolodny^{1,3}, Hagit Zer², Mor Propper², Shira Yochelis^{1,3}, Yossi Paltiel^{1,3} and Nir Keren²

6 Corresponding authors: Yossi Paltiel and Nir Keren

7 ¹Applied Physics Department, The Hebrew University of Jerusalem, Jerusalem 91904, Israel

8 ²Department of Plant and Environmental Sciences, The Alexander Silberman Institute of Life
9 Sciences, The Hebrew University of Jerusalem, Jerusalem 91904, Israel

10 ³The Center for Nanoscience and Nanotechnology, The Hebrew University of Jerusalem, Jerusalem
11 91904, Israel

12

13 Abstract

14 Photosynthetic organisms regulate energy transfer to fit to changes in environmental conditions. The
15 biophysical principles underlying the flexibility and efficiency of energy transfer in the light-harvesting
16 process are still not fully understood. Here we examine how energy transfer is regulated *in-vivo*. We
17 compare different acclimation states of the photosynthetic apparatus in a marine cyanobacterial species
18 that is well adapted to vertical mixing of the ocean water column and identify a novel acclimation
19 strategy for photosynthetic life under low light intensities. Antennae rods extend, as expected,
20 increasing light absorption. Surprisingly, in contrast to what was known for plants and predicted by
21 classic calculations, these longer rods transfer energy faster *i.e.* more efficiently. The fluorescence
22 lifetime and emission spectra dependence on temperature, at the range of 4-300K, suggests that energy
23 transfer efficiency is tuned by modifying the energetic coupling strength between antennae pigments.

24 introduction

25 Photosynthesis is regarded as one of the most efficient energy transduction processes in nature.
26 Although it rarely operates at maximum efficiency, the high quantum efficiency generates a large
27 dynamic range that allows the regulation of energy fluxes through the photosynthetic apparatus. This
28 remarkable flexibility of the photosynthetic process is critical under changing environmental conditions
29 ^{1,2}.

30 The physical mechanisms by which the energy migration is controlled in the photosynthetic apparatus
31 is under intense investigation. Traditionally, these mechanisms have been semi-classically modeled as
32 dipole-dipole interactions between adjacent chromophores using Forster resonance energy transfer
33 (FRET) amidst an incoherent bath ³. Evidence of long-lived quantum coherence, measured by 2D
34 photon-echo spectroscopy, raised the possibility that quantum phenomena may play a role in the energy
35 transfer process ^{4,5}. The nature of these coherences, whether electronic or vibronic, is still under debate
36 ⁶⁻⁹. Theoretical calculations demonstrate that both purely classic and purely quantum exciton energy
37 transfer (EET) through antenna systems have their limitations. However, a combination of quantum and
38 classic processes could enhance EET efficiency ³. The suggested combined mechanisms envision short-
39 lived coherent domains encompassing small subsets of antenna pigments. It implies that at the border
40 between classic and quantum regimes, small structural changes could have large effects on energy
41 transfer ¹⁰.

42 It is well established that the sizes of photosynthetic units can reach hundreds of pigments. A recent
43 structural study resolved an intact phycobilisome (PBS) antenna with thousands of pigments ¹¹.
44 Elucidating energy transfer dynamics in such large-scale systems will benefit from studies of intact
45 systems, within their biological context. However, the study of ultrafast processes by advanced
46 spectroscopy is usually done on isolated pigment-protein complexes. The benefits of working with
47 small numbers of pigments are clear, but the biological relevance of such experiments is limited by their
48 small scale. *In vivo* measurements present more complex scenarios that cannot be fully captured in
49 simplified isolates. As phrased by Aristotle, “which have several parts and in which the totality is not,
50 as it were, a mere heap, but the whole is something beside the parts”¹. An example for this approach is
51 the study of desiccation tolerant desert crust cyanobacteria ¹². That study demonstrated the link between
52 small changes in PBS structure and large quenching effects in the PBS antenna directly, under a
53 desiccation/rehydration scenario where water availability triggers quick energy transfer tuning. Since
54 in desert environments light intensities are high, it is interesting to also examine organisms that are
55 adapted to life where light is a limiting factor.

56 In this study we looked for an organism which is adapted to an environment where (a) light can be
57 limiting to the extreme, and (b) The intensity and quality of light varies, requiring acclimation of
58 photosynthetic systems to a broad range of light regimes. Marine *Synechococcus* spp. are obvious
59 candidates for such a study. The marine environment provides a matrix of light and environmental
60 conditions that are even more complex than those in a terrestrial desert. In the marine environment,
61 where as much as 50% of the world’s primary productivity takes place ¹³, light is the major factor
62 limiting the abundance of photosynthetic organisms. Light intensity attenuates exponentially as it
63 penetrates deeper into the water column and its spectrum is narrowed to blue (~490 nm) ^{13,14}.

64 An important perturbation of the open oceans water column is vertical mixing, which greatly affects
65 the dynamics of *Synechococcus* populations ¹⁵. Mixing of a stratified water column, typically to a depth
66 of a few hundred meters, homogeneously distributes the nutrients and the planktonic organisms along
67 the water column. The only resource that cannot be “mixed” is sunlight. As a result, an organism that
68 lives near the surface with plenty of available light, may rather abruptly find itself with very little light
69 if it reaches the deeper layers ¹⁶. The response to varying light conditions (photon flux density and
70 spectral distribution), triggers a cascade of photoacclimation responses affecting the form and function
71 of light harvesting systems ¹⁷⁻¹⁹.

72 *Synechococcus* are small unicellular coccoid cyanobacteria responsible for an estimated 25% of global
73 primary productivity. They use phycobilisomes (PBSs) as their light-harvesting antenna. Among them,
74 *Synechococcus* WH8102 represents an abundant clade that is well adapted to mixing regime and can be
75 found throughout the water column ¹⁵. Studies of marine *Synechococcus*, including WH8102,
76 demonstrated their ability to acclimate to the wide range of light intensities experienced along the water
77 column. ²⁰.

78 *Synechococcus* WH8102 PBS consist of phycobiliprotein (PBP) $\alpha\beta$ dimers organized into trimer rings
79 which, in turn, couple to create the hexamers which form the basic subunit of the core and stacked rods
80 ²¹. The core is made of allophycocyanin (APC) and the rods of phycocyanin (PC) and phycoerythrin
81 (PE). These PBPs consist of an apo-protein and contain 1-3 open-chain tetrapyrrole bilin chromophores.
82 APC and PC both bind phycocyanobilin (PCB). The different protein environments generate a
83 bathochromic shift in APC absorption ²², 620 nm in PC and 650 nm in APC. The rod extremities are
84 constituted by two structurally different forms of PE: PEI and PEII. PEI binds either only
85 phycoerythrobilin (PEB, absorption peak 545 nm), or PEB and phycourobilin (PUB, absorption peak
86 495 nm). PEII binds both PEB and PUB, but with fewer PEB than does PEI ²⁰. *Synechococcus*
87 demonstrates chromatic adaptation, able to modify the PEB into PUB and reversibly according to the
88 available light spectrum ²³⁻²⁵.

¹ Aristotle, *Metaphysics*, book VIII part 6 (350 B.C.E).

89 Importantly, *Synechococcus* WH8102 has the highest reported content of phycourobilin, the pigment
90 which best absorbs the blue light that penetrates ocean waters^{26,27}. The fact that it possesses particularly
91 large PBSs challenges energy transfer processes, since energy transfer occurs over longer distances.
92 According to classical mechanics approach, energy transfer efficiency is expected to decrease with a
93 larger number of pigments and rod length. The optimal length was calculated to be very short, on the
94 order of a few trimers²⁸.

95 Photo-physiological studies conducted on the response of marine *Synechococcus* species to light
96 intensity gradients²⁰ demonstrated a large dynamic range of photosynthetic activity. In the study we
97 present here, we take advantage of these photo-acclimation processes, to study how photosynthetic units
98 tune their energy transfer rates. Using *Synechococcus* WH8102, we generated a testing ground for
99 studying ultrafast energy transfer processes in large antennae structures with complex pigment
100 compositions *in vivo*. Our analysis includes physiological, biochemical and spectroscopic
101 measurements of energy transfer dynamics, conducted while comparing acclimated states of this marine
102 cyanobacterium to different light regimes.

103

104 Results and discussion

105 In order to compare the function of photosynthetic units within cells acclimated to light conditions
106 representing shallower and deeper water column depths, we grew *Synechococcus* WH8102 cultures
107 under blue LED light illumination, which resembles the light spectrum that penetrates the ocean
108 (Supplementary fig.1). We compared cultures grown at different blue light intensities: 10 and
109 $150 \mu\text{mol photons m}^{-2}\text{s}^{-1}$, denoted “low light” and “medium light” respectively. It is important to
110 note that in both cases the light intensity is lower than the intensity required for optimal growth, which
111 is $207 \mu\text{mol photons m}^{-2}\text{s}^{-1}$ ²⁰. Since light-induced stress was avoided, nonphotochemical
112 quenching or photo-inhibitory losses of absorbed light energy are not expected under these growth
113 conditions²⁹.

114

115 **Growth and primary productivity parameters**

116 *Synechococcus* WH8102 underwent photo-acclimation when grown under the two different blue light
117 intensities. They exhibited extensive morphological and physiological modifications, linked to changes
118 in their photosynthetic units. Immediately noticeable to the naked eye, is a change in the cultures color
119 (fig. 1A). The acclimation process is evident within two days, as seen by several physiological
120 parameters (fig. 1B, Supplementary figures 2-4) and is completed in about 7-10 days. Maximal apparent
121 photosynthetic yield, measured as Fv/Fm, shows that the low light culture exhibits significantly higher
122 values compared to the medium light culture (Table. 1), indicating higher photosynthetic capacity at
123 low light conditions in cells grown under low light.

124 *Synechococcus* WH8102 was able to grow under both low and medium light intensities. Cell numbers
125 increased at a slower rate under low light. However, unexpectedly, the side scatter area parameter (SSC-
126 A) of the fluorescence-activated cell sorting (FACS) measurement (Supplementary fig.3) raised the
127 possibility that cell sizes were larger when grown under lower light. This prompted us to examine
128 cellular morphology more closely.

129

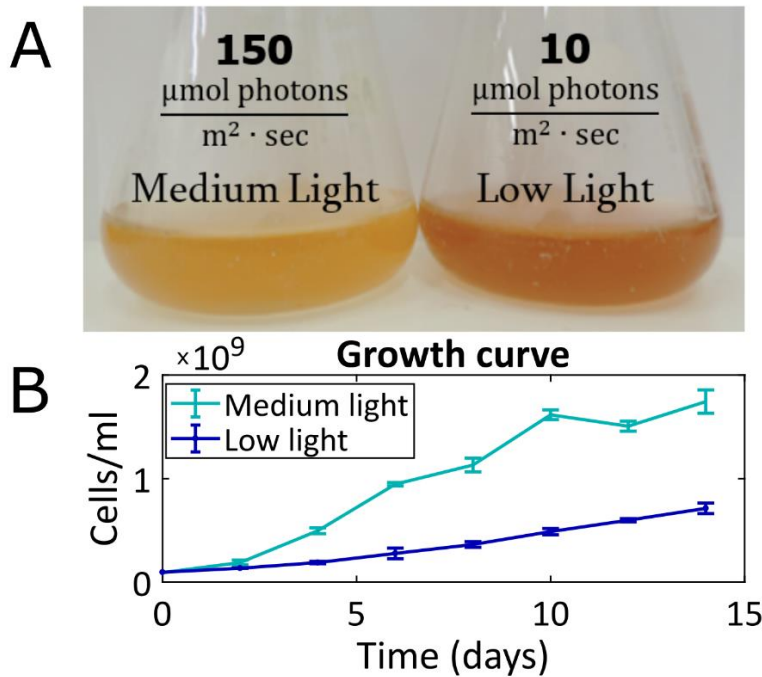


Figure 1. Photo-acclimation
(A) *Synechococcus WH8102* cultures grown under two different blue light intensities for 5 days differ in color. (B) Growth curve under different light intensities, determined by FACS. While the color of low light cultures was stronger, medium light cultures exhibited higher cell densities. SD $n=3$; The experiments were independently repeated two additional times with comparable results.

130

131

132 Cellular morphology

133 Confocal fluorescence microscopy and transmission electron microscopy (TEM) confirmed that cells
134 change their shape, size and internal structure in response to the different blue light intensities. Under
135 low light, the median size cell increased, and the size distribution was broader, as seen from the SSC-
136 A statistics (fig. 2A) and the quantification of confocal images (Supplementary fig.2). In addition, TEM
137 revealed that the cells changed their structure from round coccids under medium light to elongated
138 under low light (fig. 2B). The elongated shape of the cells under low light, along with the broad size
139 distribution, is consistent with their slower growth rate. Lastly, under medium light cells typically had
140 one thylakoid membrane while under low light three to four membranes were observed, organized in
141 uniformly distributed distances. Photosynthetic units are embedded in the thylakoid membranes, so an
142 increase in the number of membranes indicates an increase in the number of photosynthetic complexes
143 per cell. These results are similar to photo-acclimation changes observed in other marine cyanobacterial
144 species³⁰.

145 The increased cellular surface area has the advantage of a higher light absorption cross-section, which
146 is beneficial when light is limiting, provided that the energy transfer efficiency remains high. It is
147 important to note that an increase in cross-section and cell size has the disadvantage of a reduced surface
148 area per volume ratio, which may limit the assimilation of nutrients³¹. The fact that nutrients are
149 typically more abundant deeper within the ocean water column mitigates this risk. Under our
150 experimental conditions, however, nutrients were abundant in both cultures.

151

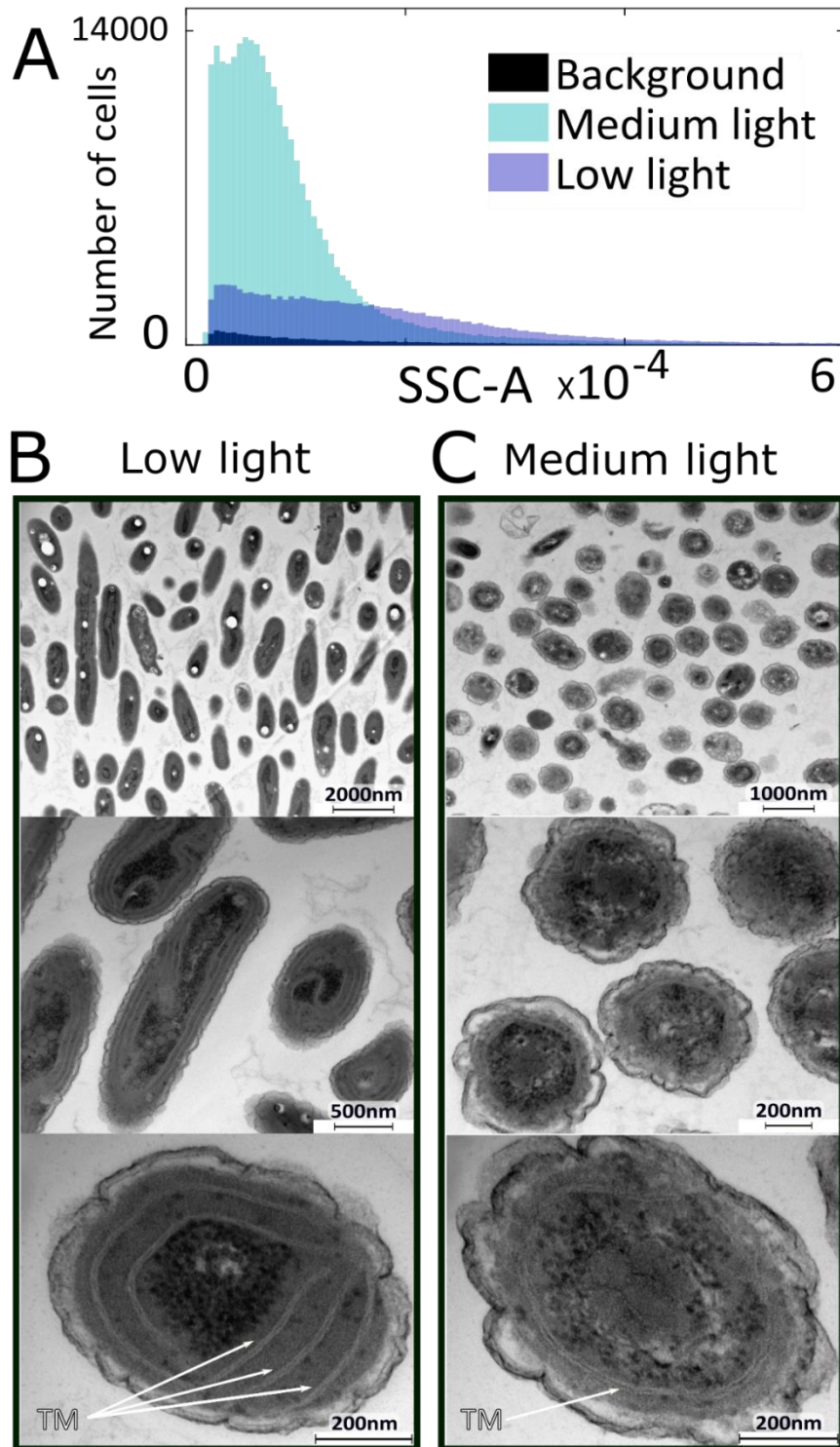


Figure 2. Cellular morphology

(A) Histogram of side scatter area (SSC-A) measured by FACS. Cultures grown under low light exhibited larger scattering values. Their mean size is about twice the size of cells grown under medium light and their scattering distribution is broader. These results indicate larger cell sizes. (B) Transmission electron microscopy of medium light cells. Typically, the cells are round, with one thylakoid membrane (TM) circling the cell. (C) Low light cells have longitude structure and contain about three thylakoid membranes. Additional information on cell sizes and architecture can be found in Supplementary fig.2.

152

153

154 **Photosynthetic complexes**

155 As implied by the higher number of thylakoid membranes, under low light the number of photosynthetic
 156 units is higher. This is supported by the fact that chlorophyll *a* absorption, a component of both
 157 photosystems, was increased 8 folds at low light as compared to medium light on a per-cell basis (fig.
 158 3). Similarly, on a protein basis, chlorophyll content increased 7.4 folds (Table 1). The ratio of PSI to
 159 PSII was slightly increased under low light, as demonstrated by protein immunoblotting
 160 (Supplementary fig.5). A prominent change is also evident in the composition of the photosynthetic
 161 antennae pigments. Examining the pigment content of the antenna, our results show that under low
 162 light, the PE content increases. The ratios between the different pigments change, as seen in table 1.
 163 Specifically, the ratios of PUB and PEB to PC absorption increase approximately two folds. These
 164 results are comparable to a previous study done on *Synechococcus* WH8102²⁰.

165

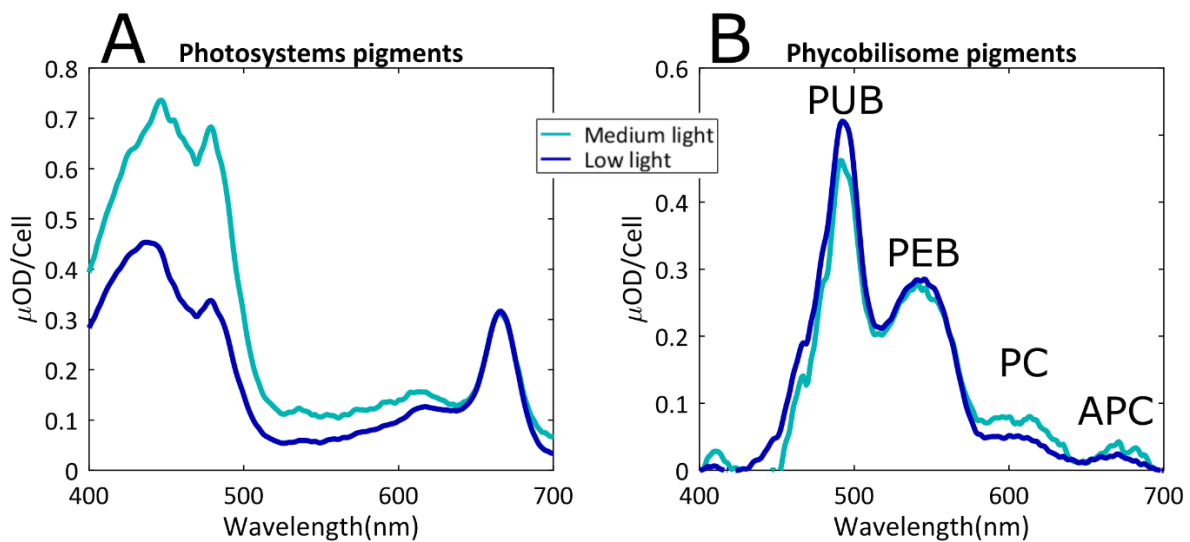


Figure 3. Photosynthetic complexes content

Absorption spectra of extracted pigments from the cells measured using integrating sphere. Values are normalized on a per cell basis. Low light cells contained considerably more pigments and their data was divided by eight to fit on the same scale. (A) Methanol extraction solubilizing hydrophobic chlorophylls and carotenoids. Since chlorophyll has two absorption peaks and the first excited state absorption is equal, the difference in the absorption between 450-500nm is a result of a larger quantity of carotenoids in medium light. (B) MTN solubilized pigments showing the phycobilisome pigments (phycobilins). Lower light has higher PUB:PEB but lower PC:PEB ratio. In-vivo absorption spectra appears in Supplementary fig.6.

166

167

	Low Light	Medium Light	LL/ML ratio
Chl/protein ($\mu\text{g chl mg}^{-1}\text{protein}$)	274	37	7.4
PUB/PC	11.9 ± 1.5 ($n = 4$)	4.9 ± 1.5 ($n = 4$)	2.4
PEB/PC	6.2 ± 0.9 ($n = 4$)	2.9 ± 0.8 ($n = 4$)	2.1
Fv/Fm	0.43 ± 0.04 ($n = 2$)	0.22 ± 0.03 ($n = 2$)	1.9

Table 1. Differences in the photosynthetic units' composition and function (n – number of independent repeats).

168

169

170

171 PBSs increase in size under low light³². Absence of PC rod linker (LR) genes such as *cpcC* or *cpcD* in
172 *Synechococcus* WH8102 suggests that under all light conditions there is only one hexameric PC disk
173 per PBS rod^{32,33}. Taking this into account, it is most likely that under low light, where proportions of
174 PUB and PEB to PC are higher, the rods become longer. According to Six and co-workers³² PEII varies
175 more than PEI, therefore it is reasonable to conclude that the number of PEII disks in each rod is higher
176 under low light than under medium light. These considerations generated the model presented in fig. 4.
177 Similar structures were suggested in studies of other *Synechococcus* specie³⁴.

178 These structures raise an interesting problem. While bigger light harvesting antennae containing
179 additional PUB have an increased absorption cross-section, they generate a longer pathway for energy
180 transfer to the reaction centers. Theoretical models using FRET demonstrated that an increase in rod
181 length is expected to result in lower energy transfer efficiency²⁸. However, we found the functionality
182 of each photosynthetic unit is improved under low light, as seen from the maximal apparent
183 photosynthetic yield (F_v/F_m) values. To further probe the issue of energy transfer efficiency, we
184 examined fluorescence spectra and lifetime characteristics.

185

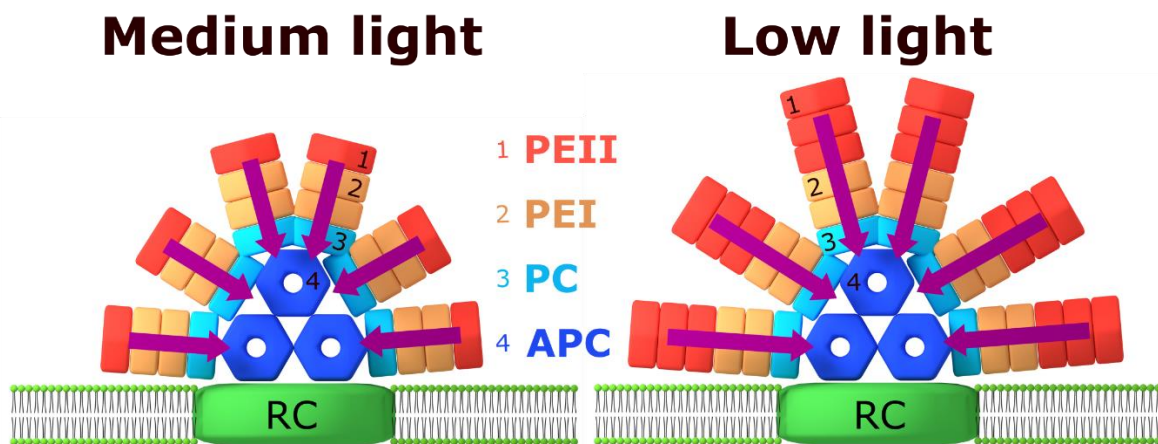


Figure 4. PBS structure under different light intensities. Suggested PBS scheme, showing the differences between the complexes grown under low versus medium light. Under low light the PBS is larger, with longer rods that have additional PEII hexamers (with higher PUB content). Energy absorbed at the extremities travels longer distance to the reaction centers (RCs). Structures are based on the pigment ratios found in this study as well as in Six and co-workers³² and the structural organization of PBS in other strains that was published before³⁴, suggesting it is typically comprised of three APC cylinders and six rods.

186

187 Energy transfer properties

188 Steady state fluorescence spectra of *Synechococcus* WH8102, at room temperature, allow us to compare
189 the energy flow through the photosynthetic apparatus. Fig. 5A shows the emission spectra of cultures
190 treated with DCMU, a PSII electron transfer inhibitor. It allows us to eliminate photochemistry and
191 concentrate on exciton energy transfer to the reaction center. Excitation was set at 497 nm, the
192 absorption peak of the PUB at the extremity of the rod. The spectra were normalized to the emission at
193 652 nm, the peak of the PC (assuming only one PC disk per rod). Interestingly, the emission in the
194 spectral range of PC, APC and PSII is identical for both cultures (650-700 nm). This implies that the
195 cells have maintained energy transfer homeostasis by regulating energy flow, so that the same flux that
196 passes through the PC discs reaches the reaction center under both low and medium light.

197 The emission peak of the PE was shifted (565 nm at low light, 572 nm at medium light), consistent with
198 the higher PUB:PEB ratio under low light (fig. 3). Moreover, PE emission was more than twice stronger
199 in low light. This is expected considering the higher PE content. It may also imply that multiple PE
200 units on the same rod cannot move energy simultaneously through the single PC disk, or that some of
201 the PE pigments in cells grown under low light are not strongly coupled. A small number of uncoupled
202 pigments can have a large contribution to the fluorescence yield.

203 To further investigate the rate of energy transfer following excitation of PUB, we performed
204 measurements of the excited state's lifetime. Time-correlated single photon counting approach
205 (TCSPC) was used to measure the decay lifetime of the different components of the photosynthetic unit.
206 Excitation was set at 485 nm targeting the extremities of the PBS rod, and emission was collected in
207 three spectral windows, covering the phycobilins (PBS window, 500-675 nm), the APC terminal emitter
208 and photosystem chlorophylls (PS window, 675 to 750 nm), and the overall system's lifetime (Wide
209 window, 500 to 750 nm). The measured lifetime, τ , is the typical lifetime of the system's excited state,
210 and is composed of different pathways which can be related to three major components: radiative (τ_R),
211 heat dissipation (τ_k) and energy transfer (τ_{ET}) pathways. Their combined effective value is formulated
212 as a harmonic average $\frac{1}{\tau} = \frac{1}{\tau_R} + \frac{1}{\tau_k} + \frac{1}{\tau_{ET}}$.

213 The PBS average lifetime was 0.12 ns under medium light, compared to 0.09 ns under low light, at
214 room temperature (Fig. 5B). The fact that the lifetime is shortened under lower light is surprising. The
215 opposite phenomenon was reported in plants, where lower light triggered an increase in lifetime³⁵. The
216 shorter lifetime indicates that in each photosynthetic unit, the absorbed energy decays faster. This could
217 either be due to higher dissipation of the energy, or due to faster energy transfer rate. The light intensity
218 is low in both cases; therefore, multi-exciton processes are not relevant. Fv/Fm values are higher in low
219 light acclimated cells, making disorder dissipation (energy quenching) by coupling to environment less
220 probable¹⁰. We hypothesized that higher energy transfer rates are responsible for the shorter life time.

221 The 90 ps shift between the peak of the PBS window trace and the PS window trace (fig. 5B insert)
222 gives a rough estimation of the transfer rate between the phycobilisome and the reaction center. The
223 fact that this timing is similar for both samples although the number of pigments per system is different
224 supports the hypothesis that PBS energy transfer is accelerated under low light. The PS lifetime was
225 0.25 ns under medium light compared to 0.35 ns under low light. Examining the components of these
226 decay curves indicates that the contribution of the fast decay component in the medium light is larger.
227 This may be a result of the direct excitation of photosystem chlorophylls. While chlorophyll *a*
228 absorption peak is around 430 nm, they do absorb, with lower efficiency, also at 497 nm (Fig. 3). Under
229 medium light where chlorophyll absorption is not as masked by PBS absorption as in low light, the
230 proportion of direct chlorophyll excitation will be higher.

231 As expected from the similar PC/PSII steady-state emission ratio but different PE/PC ratio seen in fig
232 5A, the major difference in the lifetime between the two samples is evident in the PBS fluorescence
233 lifetime, suggesting this is the energy transfer step that is enhanced.

234 Fig. 5C shows that at 5K, where contributions of thermal vibrations are negligible, the lifetime at low
235 light is still shorter. In fact, the difference in lifetimes increases with decreasing temperatures (Fig.
236 6A). Since radiation decay rates are intrinsic, it implies the energy transfer from the PBS rod
237 extremity (the PUB) is indeed faster. This finding is surprising. FRET calculations predict a decrease
238 with increasing number of pigments²⁸. Such a decrease was indeed demonstrated in plant systems,
239 where longer lifetimes were reported in the large antenna of low light acclimated samples³⁵.

240

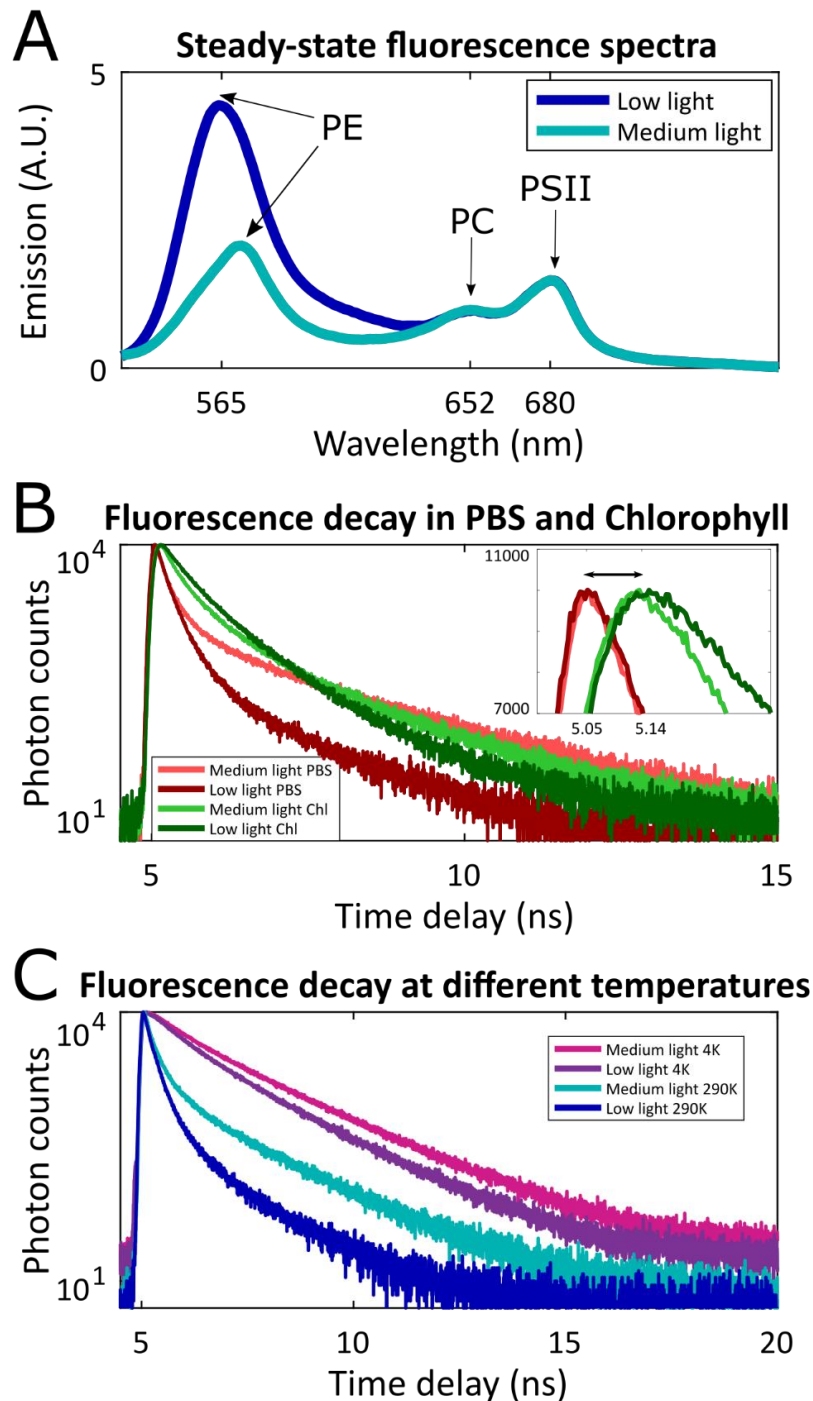


Figure 5. Energy transfer in photosynthetic apparatus. (A) *in vivo* emission spectra (excitation 497 nm). Emission was normalized to the peak of phycocyanin (652 nm). Samples treated with 5 μ M DCMU, to inhibit PSII photochemistry. PSI fluorescence is not observed at room temperature. The measurements were repeated in four independent experiments with comparable results. (B) Time resolved fluorescence spectroscopy *in vivo* (excitation at 485 nm, absorbed mainly by PE). Emission was collected in spectral windows of 500-675 nm (PBS window) or 675-750 nm (mainly chlorophyll, PS window). Insert shows the rise time of the chlorophyll peak. In both low and medium light, a 90 ps delay between the PS window and the PBS windows was observed. (C) Time resolved fluorescence at two temperatures (4K and 290K). Emission was integrated over both windows (500-750 nm).

241

242

243 **Pigment coupling**

244 We hypothesized that faster energy transfer over a larger pigment system will require stronger energetic
245 coupling between these pigments. To explore this hypothesis and inspect the coupling strength between
246 the pigments, we measured the temperature dependence of both steady state and time-resolved
247 fluorescence, from 300K down to 4K. Photochemistry is blocked below freezing at ~273K, though the
248 photosynthetic complexes remain intact. Spectral characteristics of a multi-chromophoric system are
249 governed by the coupling between the chromophores, which, in turn, is affected by thermal vibrations.
250 Hence, the temperature dependence of the lifetime and the emission spectrum can be used as a probe to
251 study the coupling regime between pigments in the photosynthetic apparatus. This approach already
252 produced interesting results *in vitro*³⁶, here we use it *in vivo*.

253 Fig. 6A shows the average fluorescence lifetime as a function of temperature. An interesting feature is
254 the abrupt rise in lifetime at the temperature range of 250-265K. This phenomena was reported *in vitro*
255 in isolated phycobiliproteins³⁷. It was related to photoisomerization of the billins into a form more
256 prone to quenching, due to interactions of the solvent with the chromophores that are influenced by
257 temperature. Maksimov and co-workers reasoned that the interaction between monomeric subunits of
258 phycobiliprotein trimers prevents photoisomerization of the chromophores. Once this interaction is
259 weakened due to the decrease in temperature, photoisomerization takes place. In our case the
260 measurement was done *in vivo*, where linker proteins occupy the center of the trimer. Nevertheless, we
261 were able to detect this anomaly in intact cell samples. The *in vivo* temperature anomaly had a different
262 trend in medium and low light cells. While in medium light cells the rise began immediately upon
263 cooling, low light grown cells maintained a constant lifetime down to lower temperatures (to about
264 280K), and their rise in lifetime is more gradual. According to the proposed explanation for the rise in
265 lifetime, this difference indicates stronger interaction between the chromophores in the low light grown
266 PBS, supporting our hypothesis.

267 Fig. 6B and fig. 6C show the emission spectra at a few chosen temperatures as a function of temperature.
268 In both medium and low light cells, emission intensity increases dramatically with the decrease in
269 temperature, as expected when decreasing the heat dissipation component. The main difference was the
270 change in the ratio between the PUB emission (560 nm) to PEB emission (574 nm). At room
271 temperature, the emission of both pigments comprised one visible peak due to thermal broadening. At
272 lower temperatures, the two spectral lines narrowed and the emissions of the two pigments were
273 resolved. While under low light the PUB:PEB emission peaks ratio decreases significantly with
274 temperature (down to 0.45 at 5K), under medium light the ratio is closer to 1 (reaching 0.8 at 5K). Since
275 the PUB and PEB content remained constant while cooling down, it implies that under low light a larger
276 fraction of the energy absorbed by PUB was transferred to PEB and emitted from PEB, even at 5K,
277 proving stronger coupling between the PUB-PEB pigments. It is interesting to note that the PBS under
278 low light has a higher PUB:PEB ratio (as inferred from fig. 3 and illustrated in fig. 4). In other words,
279 even though the PUB content under low light is higher, we observe less PUB emission than in medium
280 light. These results further support the hypothesis that in cells acclimated to low light, the coupling
281 between the chromophores in the PBS is stronger. The stronger coupling leads to the higher energy
282 transfer rate.

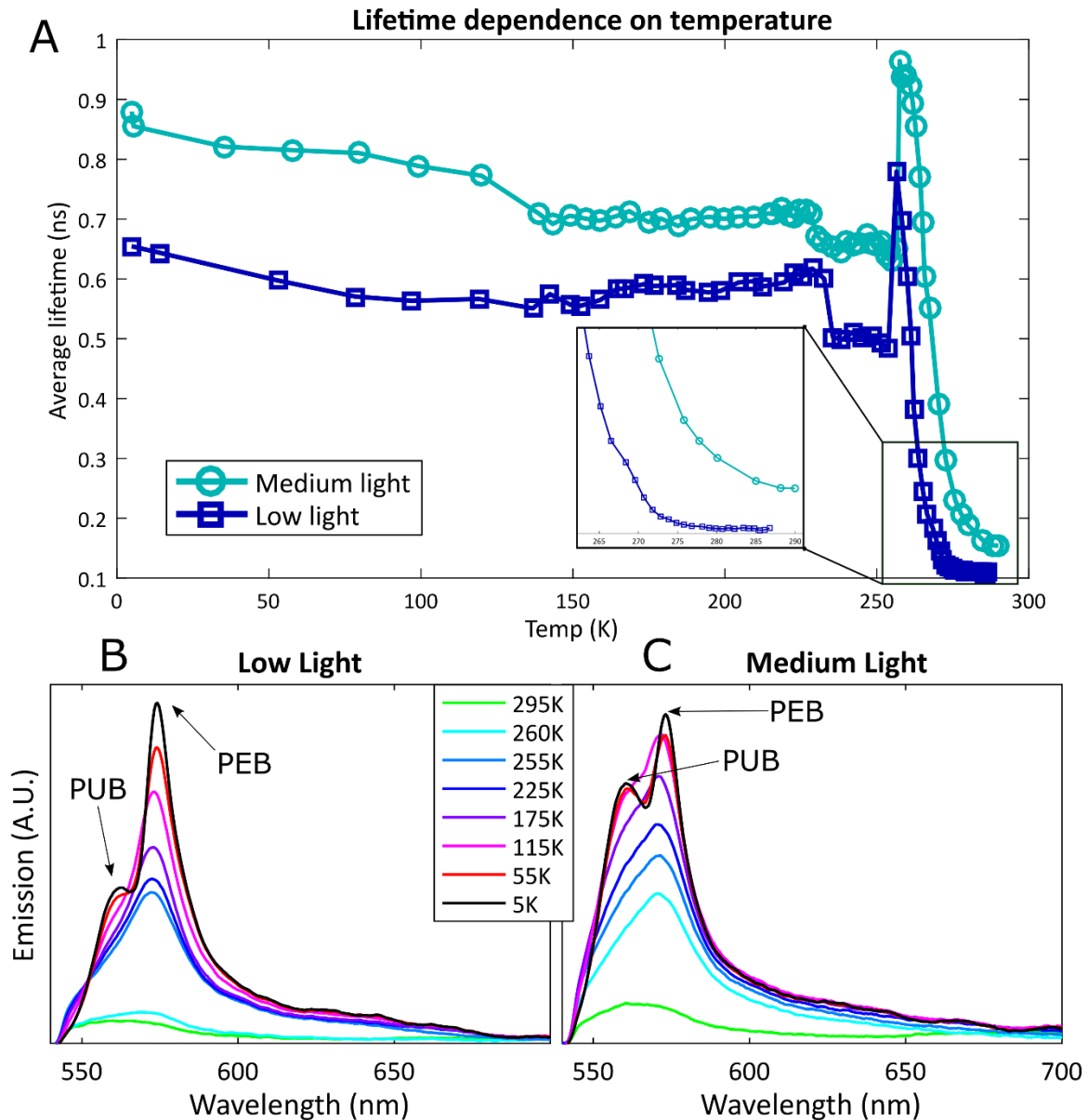


Figure 6. Temperature dependence. (A) Average lifetime of the photosynthetic complex as a function of temperature (measurement parameters as in 5C). (B,C) Fluorescence dependence on temperature. Spectrally resolved emission, following excitation at 450 nm, as a function of temperature from 295 down to 5K. Several representative temperatures are shown on graph.

283

284

285 **Conclusions**

286 Taking advantage of the extensive photo-acclimation capacity of *Synechococcus* WH8102, we were
287 able to study physical mechanisms governing the acclimation of the photosynthetic apparatus. Cells
288 displayed extreme morphological flexibility, acclimating to the irradiance regime within days. When
289 experiencing low blue light, growth rates were slower, cells were bigger and contained more thylakoid
290 membranes. The number of photosynthetic units increased, but what we find most fascinating is that
291 each of these units was more efficient under a low light regime.

292 The PBS was bigger under low light, with longer rods containing additional PUB pigments which
293 increase the absorption cross-section at 495 nm. Surprisingly, instead of decreasing the rate of energy
294 transfer, as was reported in plant systems³⁵, the longer rods exhibit faster energy transfer, as seen by

295 the shorter lifetime measured as a function of temperature. Several lines of evidence support the
296 hypothesis that improved energy transfer is achieved by stronger coupling between the pigments.
297 Coupling strength according to the semi-classical FRET theory is a function of dipole strength,
298 distances, orientation and energetic overlap between the pigments in the exciton transfer network.
299 Increased efficiency over a larger pigment network suggests the involvement of coupling that is stronger
300 than predicated by FRET calculations. While it is too early to pinpoint the exact energy transfer
301 mechanism, the photo-acclimation response studied here is a step towards a better understanding of
302 these processes. Unveiling the mechanism by which cyanobacteria tune energy transfer will help
303 understand photo-acclimation, and may pave the way to bio-inspired nano-scale energy-transducing
304 devices with a broad dynamic range.

305

306 Materials and Methods

307 **Growth conditions and cellular morphology measurements**

308 *Synechococcus* WH8102 cultures were grown in ASW medium under continuous blue light (spectrum
309 in Supplementary fig.1), in 10 and 150 $\mu\text{mol photons m}^{-2}\text{s}^{-1}$, referred to as “low light” and “medium
310 light” respectively. For FACS analysis, one ml samples were collected every second day, preserved in
311 0.2% glutaraldehyde grade II (Sigma), frozen in liquid nitrogen and stored at -80°C . Cells were counted
312 using FACS Aria III flow cytometer-sorter (BD Biosciences, San Jose, CA) using 488nm laser. The
313 flow rate was $14 \mu\text{l min}^{-1}$, data was collected for 1 min. Confocal microscopy was performed using an
314 Olympus FV-1200 confocal microscope Olympus, Japan. For transmission electron microscopy (TEM),
315 cells were harvested by centrifugation at 8000g for 5 min, washed twice in ASW and chemically fixed
316 in 2% paraformaldehyde and 2.5% Glutaraldehyde in 0.1M Cacodylate buffer (pH 7.4). Sample
317 preparation followed standard procedures. Sections were sequentially stained with Uranyl acetate and
318 Lead citrate for 3 minutes each and viewed with Tecnai 12 TEM 100kV (Phillips, Eindhoven, the
319 Netherlands) equipped with MegaView II CCD camera.

320 **Physiological parameters, pigment and protein composition**

321 Oxygen Evolution was measured using Clark-type electrode (Hansatech Instruments Ltd, King’s
322 Lynn, Norfolk, UK). Measurements were performed using the same blue LED illumination under
323 which the sample grew. Light intensities were altered by changing the distance of the light source
324 from the culture and by using ND filters for attenuation. Chlorophyll fluorescence kinetic parameters
325 were measured using a PAM 2500 (Walz, Effeltrich, Germany). Fm was measured following the
326 addition of DCMU under actinic light.

327 Hydrophobic pigments were extracted in 100% methanol and the pellet containing hydrophilic
328 phycobilins was suspended in TMN.

329 **Spectroscopic measurements**

330 Steady state Absorption and Fluorescence were performed within an integrated sphere to reduce
331 scattering, using a Horiba PTI Quantamaster (Kyoto, Japan).

332 Temperature dependent time-resolved fluorescence measurements were carried out using a time-
333 correlated single-photon counting (TCSPC) setup built on attoDRY800 cryo-optical table. Excitation
334 was done with a Finaium WhiteLase SC-400 supercontinuum laser monochromatized at 485 nm at a
335 repetition rate of 40MHz. Detected with MPD PD-100-CTE-FC photon counter and PicoHarp300.
336 The samples were trapped between two sapphire windows with a Teflon O-ring in between, in their
337 original medium with no additives. This sample holder was put inside a vacuum chamber, thermally
338 coupled to a cold plate that is gradually cooled down to 4 k. Sample temperature was measured along
339 the process with a Cernox DT-670-SD attached to the sapphire window. There may be an offset of up

340 to a few degrees between the temperature recorded by the sensor and the actual temperature of the
341 sample. Lifetime data was fitted using DecayFit 1.4 software and a three exponential decay model.

342 Temperature dependent emission spectra were recorded at the same cryogenic setup: excited with a
343 CPS450nm laser diode and emission detected with Flame spectrometer by Oceanview.

344

345 1. Mullineaux, C. W. Electron transport and light-harvesting switches in cyanobacteria. *Front.*
346 *Plant Sci.* **5**, 7 (2014).

347 2. Croce, R. & van Amerongen, H. Natural strategies for photosynthetic light harvesting. *Nat.*
348 *Chem. Biol.* **10**, 492–501 (2014).

349 3. Chenu, A. & Scholes, G. D. Coherence in Energy Transfer and Photosynthesis. *Annu. Rev.*
350 *Phys. Chem.* **66**, 69–96 (2015).

351 4. Collini, E. *et al.* Coherently wired light-harvesting in photosynthetic marine algae at ambient
352 temperature PCB-158 PCB-82 DBV dimer MBV A MBV B PCB D PCB C PCB C PCB D d
353 2.0 Energy (eV) 2.2 2.4 2.6. **463**, (2010).

354 5. Engel, G. S. *et al.* Evidence for wavelike energy transfer through quantum coherence in
355 photosynthetic systems. **446**, (2007).

356 6. Caruso, F., Chin, A. W., Datta, A., Huelga, S. F. & Plenio, M. B. Highly efficient energy
357 excitation transfer in light-harvesting complexes: The fundamental role of noise-assisted
358 transport. *J. Chem. Phys.* **131**, 105106 (2009).

359 7. Mohseni, M., Rebentrost, P., Lloyd, S. & Aspuru-Guzik, A. Environment-assisted quantum
360 walks in photosynthetic energy transfer. *J. Chem. Phys.* **129**, 174106 (2008).

361 8. Ma, F., Romero, E., Jones, M. R., Novoderezhkin, V. I. & van Grondelle, R. Both electronic
362 and vibrational coherences are involved in primary electron transfer in bacterial reaction
363 center. *Nat. Commun.* **10**, 933 (2019).

364 9. Duan, H.-G. *et al.* Nature does not rely on long-lived electronic quantum coherence for
365 photosynthetic energy transfer. *Proc. Natl. Acad. Sci. U. S. A.* **114**, 8493–8498 (2017).

366 10. Keren, N. & Paltiel, Y. Photosynthetic Energy Transfer at the Quantum/Classical Border.
367 *Trends Plant Sci.* **23**, 497–506 (2018).

368 11. Zhang, J. *et al.* Structure of phycobilisome from the red alga *Griffithsia pacifica*. *Nature* **551**,
369 57–63 (2017).

370 12. Bar, L. *et al.* Changes in aggregation states of light-harvesting complexes as a mechanism for
371 modulating energy transfer in desert crust cyanobacteria. **700**, (2017).

372 13. Falkowski, P. G., & Raven, J. A. *Aquatic photosynthesis*. (Princeton University Press, 2013).

373 14. Eyal, G. *et al.* *Euphyllia paradivisa*, a successful mesophotic coral in the northern Gulf of
374 Eilat/Aqaba, Red Sea. *Coral Reefs* (2016). doi:10.1007/s00338-015-1372-1

375 15. Post, A. F. *et al.* Long Term Seasonal Dynamics of *Synechococcus* Population Structure in the
376 Gulf of Aqaba, Northern Red Sea. *Front. Microbiol.* **2**, 131 (2011).

377 16. Carlson, D. F., Fredj, E. & Gildor, H. The annual cycle of vertical mixing and restratification
378 in the Northern Gulf of Eilat/Aqaba (Red Sea) based on high temporal and vertical resolution
379 observations. *Deep Sea Res. Part I Oceanogr. Res. Pap.* **84**, 1–17 (2014).

380 17. Falkowski, P. G. & LaRoche, J. ACCLIMATION TO SPECTRAL IRRADIANCE IN
381 ALGAE. *J. Phycol.* **27**, 8–14 (1991).

382 18. Grébert, T. *et al.* Light color acclimation is a key process in the global ocean distribution of

- 383 Synechococcus cyanobacteria. *Proc. Natl. Acad. Sci. U. S. A.* **115**, E2010–E2019 (2018).
- 384 19. Gutu, A. & Kehoe, D. M. Emerging Perspectives on the Mechanisms, Regulation, and
385 Distribution of Light Color Acclimation in Cyanobacteria. *Mol. Plant* **5**, 1–13 (2012).
- 386 20. Six, C., Thomas, J. C., Brahamsha, B., Lemoine, Y. & Partensky, F. Photophysiology of the
387 marine cyanobacterium *Synechococcus* sp. WH8102, a new model organism. *Aquat. Microb.
388 Ecol.* **35**, 17–29 (2004).
- 389 21. Adir, N. *Elucidation of the molecular structures of components of the phycobilisome:
390 reconstructing a giant.*
- 391 22. Stirbet, A., Lazár, D., Papageorgiou, G. C. & Govindjee. *Chlorophyll a Fluorescence in
392 Cyanobacteria: Relation to Photosynthesis.* *Cyanobacteria* (2019). doi:10.1016/B978-0-12-
393 814667-5.00005-2
- 394 23. Shukla, A. *et al.* Phycoerythrin-specific bilin lyase-isomerase controls blue-green chromatic
395 acclimation in marine *Synechococcus*. doi:10.1073/pnas.1211777109
- 396 24. Sanfilippo, J. E. *et al.* Self-regulating genomic island encoding tandem regulators confers
397 chromatic acclimation to marine *Synechococcus*. doi:10.1073/pnas.1600625113
- 398 25. Mahmoud, R. M. *et al.* Adaptation to Blue Light in Marine *Synechococcus* Requires MpeU, an
399 Enzyme with Similarity to Phycoerythrobilin Lyase Isomerases. *Front. Microbiol.* **8**, 243
400 (2017).
- 401 26. Fuller, N. J. *et al.* Clade-Specific 16S Ribosomal DNA Oligonucleotides Reveal the
402 Predominance of a Single Marine *Synechococcus* Clade throughout a Stratified Water Column
403 in the Red Sea. *Appl. Environ. Microbiol.* **69**, 76 (2003).
- 404 27. Toledo, G., Palenik, B. & Brahamsha, B. *Swimming Marine Synechococcus Strains with
405 Widely Different Photosynthetic Pigment Ratios Form a Monophyletic Group.* *APPLIED AND
406 ENVIRONMENTAL MICROBIOLOGY* **65**, (1999).
- 407 28. Chenu, A. *et al.* Light Adaptation in Phycobilisome Antennas: Influence on the Rod Length
408 and Structural Arrangement. *J. Phys. Chem. B* **121**, 9196–9202 (2017).
- 409 29. Soitamo, A., Havurinne, V. & Tyystjärvi, E. Photoinhibition in marine picocyanobacteria.
410 *Physiol. Plant.* **161**, 97–108 (2017).
- 411 30. Kana, T. M. & Glibert, P. M. *Synechococcus WH7803-I. Growth, pigmentation, and cell
412 composition.* **34**,
- 413 31. Lis, H., Shaked, Y., Kranzler, C., Keren, N. & Morel, F. M. Iron bioavailability to
414 phytoplankton: an empirical approach. *ISME J.* **9**, 1003–1013 (2015).
- 415 32. Six, C. *et al.* Two Novel Phycoerythrin-Associated Linker Proteins in the Marine. *J. Bacteriol.*
416 **187**, 1685–1694 (2005).
- 417 33. Palenik, B. *et al.* The genome of a motile marine *Synechococcus*. *Nature* **424**, 1037–1042
418 (2003).
- 419 34. Arteni, A. A., Ajlani, G. & Boekema, E. J. Structural organisation of phycobilisomes from
420 *Synechocystis* sp. strain PCC6803 and their interaction with the membrane. *Biochim. Biophys.
421 Acta - Bioenerg.* **1787**, 272–279 (2009).
- 422 35. Wientjes, E., Van Amerongen, H. & Croce, R. Quantum Yield of Charge Separation in
423 Photosystem II: Functional Effect of Changes in the Antenna Size upon Light Acclimation The
424 migration of LHCII from PSII to PSI has. *J. Phys. Chem. B* **117**, 51 (2013).
- 425 36. Chmeliov, J. *et al.* The nature of self-regulation in photosynthetic light-harvesting antenna.
426 16045 (2016). doi:10.1038/NPLANTS.2016.45

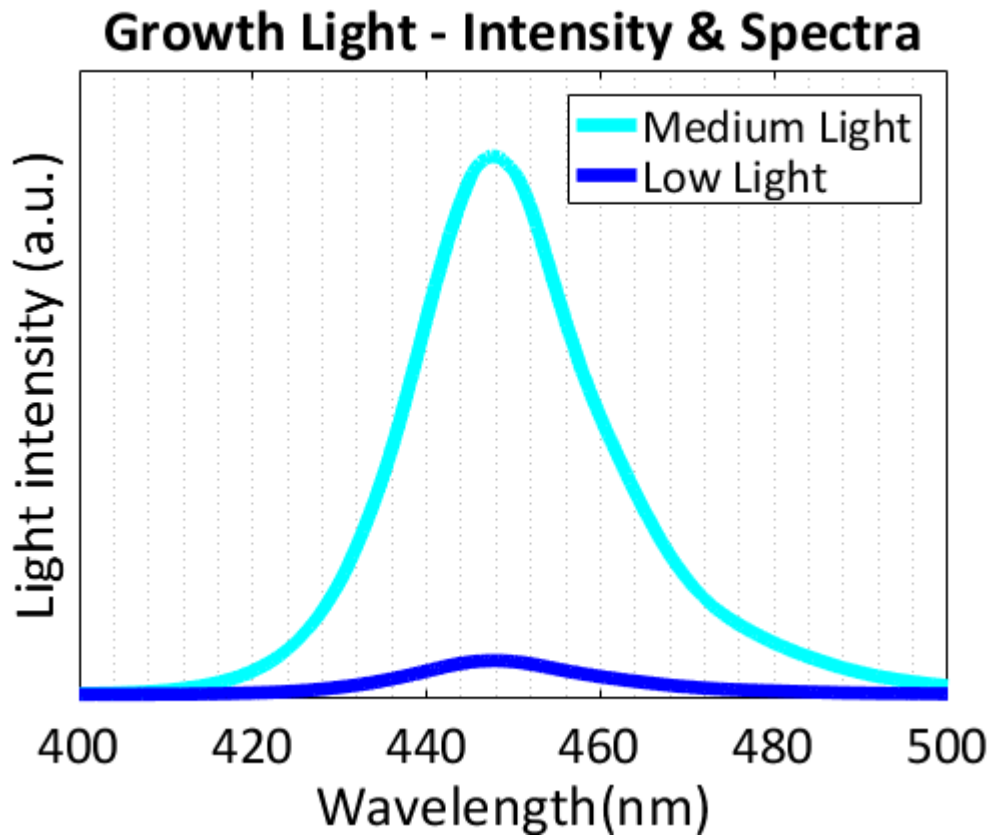
- 427 37. Maksimov, E. G. *et al.* Anomalous temperature dependence of the fluorescence lifetime of
428 phycobiliproteins. *Laser Phys. Lett.* **10**, 055602 (2013).
429
430

431

Supplementary Information

432

433



434

435 **Fig. S1.** Spectra of LED illumination under which the bacteria cultures were grown. Medium light is
436 150 and low light is 10 $\mu\text{mol photons m}^{-2}\text{s}^{-1}$. The spectra resembles the spectra found within the
437 water column.

438

439

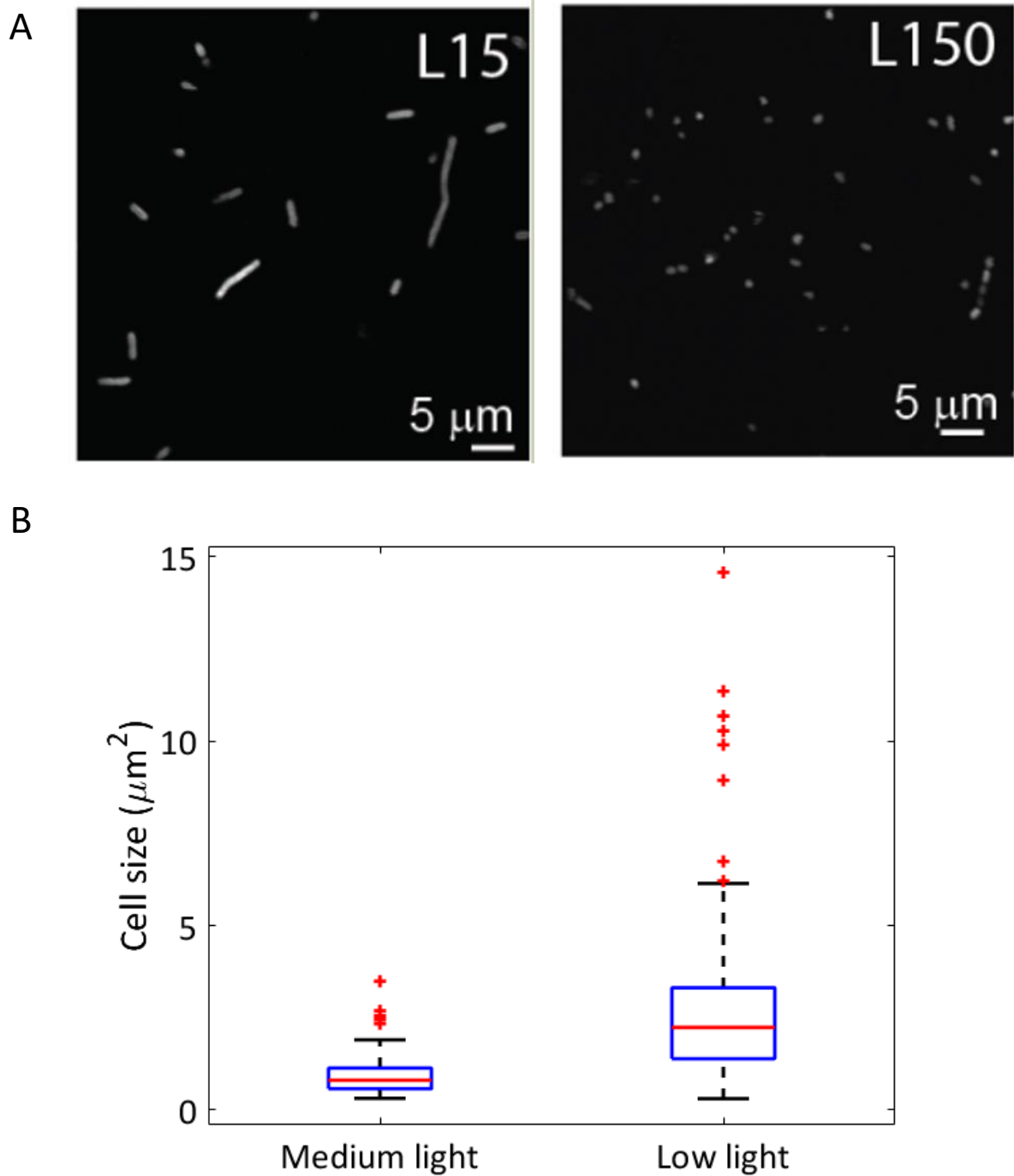


Fig. S2. (A) Fluorescence confocal imaging of low light (L15) and medium light (L150) grown cells. (B) Quantification of cell sizes from confocal microscopy images. The box plot central mark indicates the median, the bottom and top edges of the box indicate the 25th and 75th percentiles. The whiskers extend to the most extreme data points not considered outliers, shown as red pluses.

440

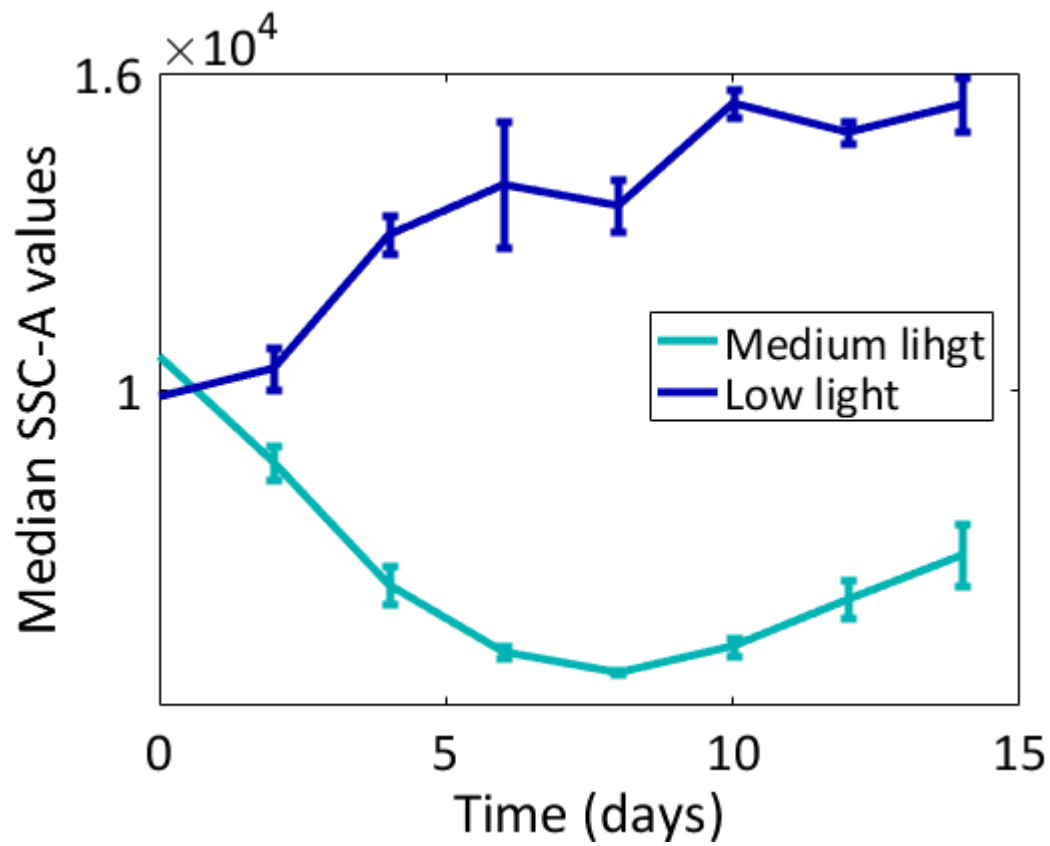
441

442

443

444

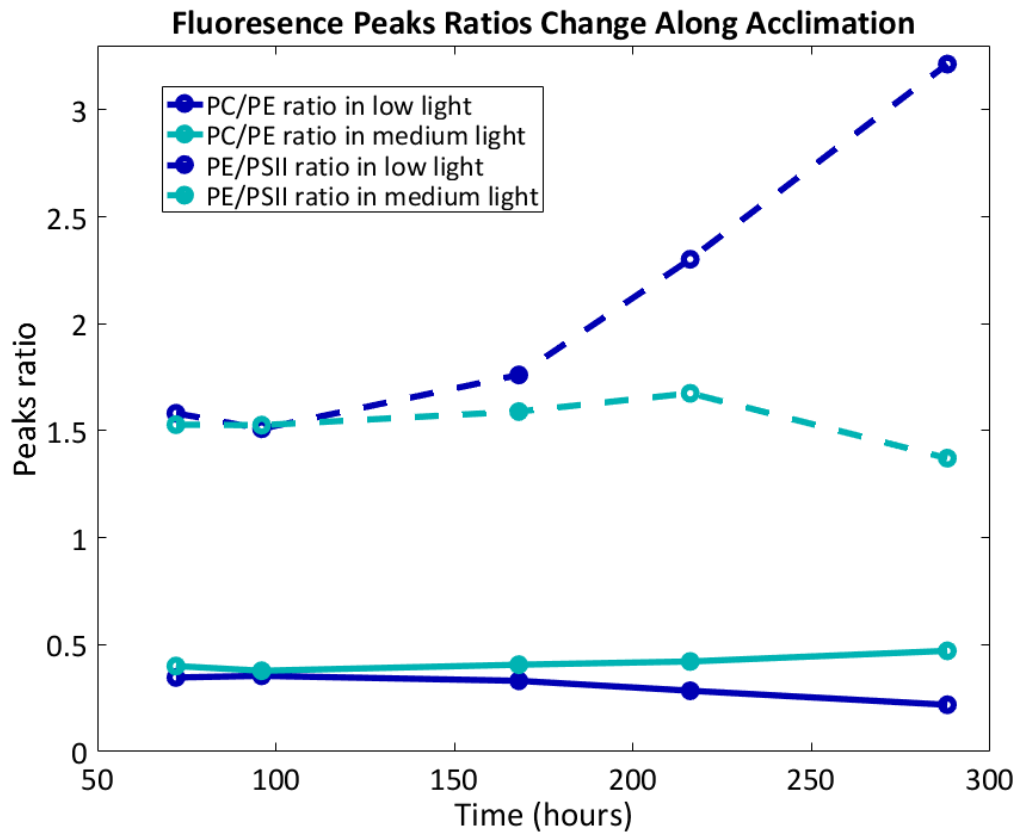
445



446

447 **Fig. S3.** Progression of changes in SSC-A Median values. Averages and SD were derived from three
448 independent cultures.

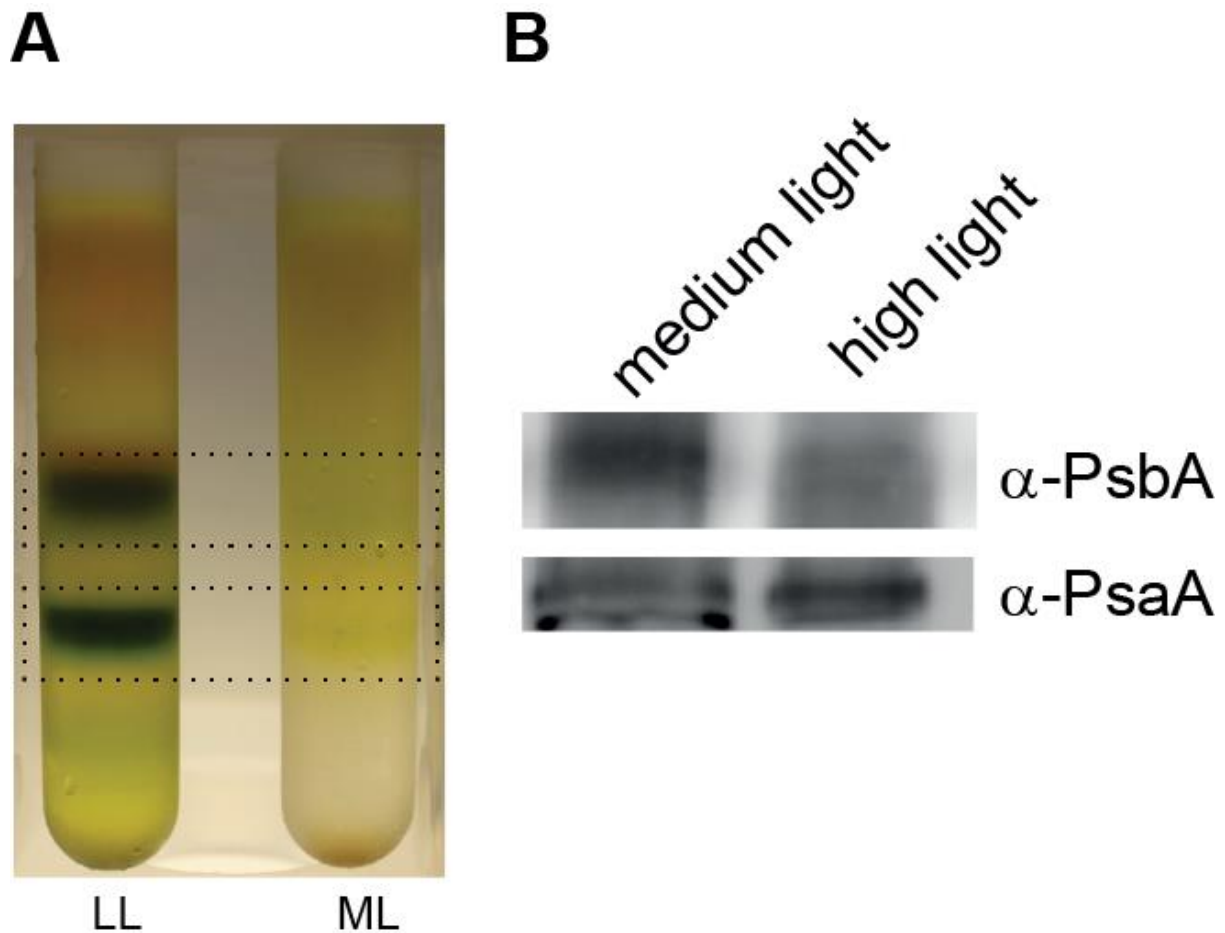
449



450

451 **Fig S4.** Fluorescence spectra following excitation at 497 nm were recorded along the acclimation
452 process. The ratios between the different pigments' peaks change along the process. Cultures were
453 treated with 5 mM DCMU prior to measurement to allow better comparison of PSII emission.

454

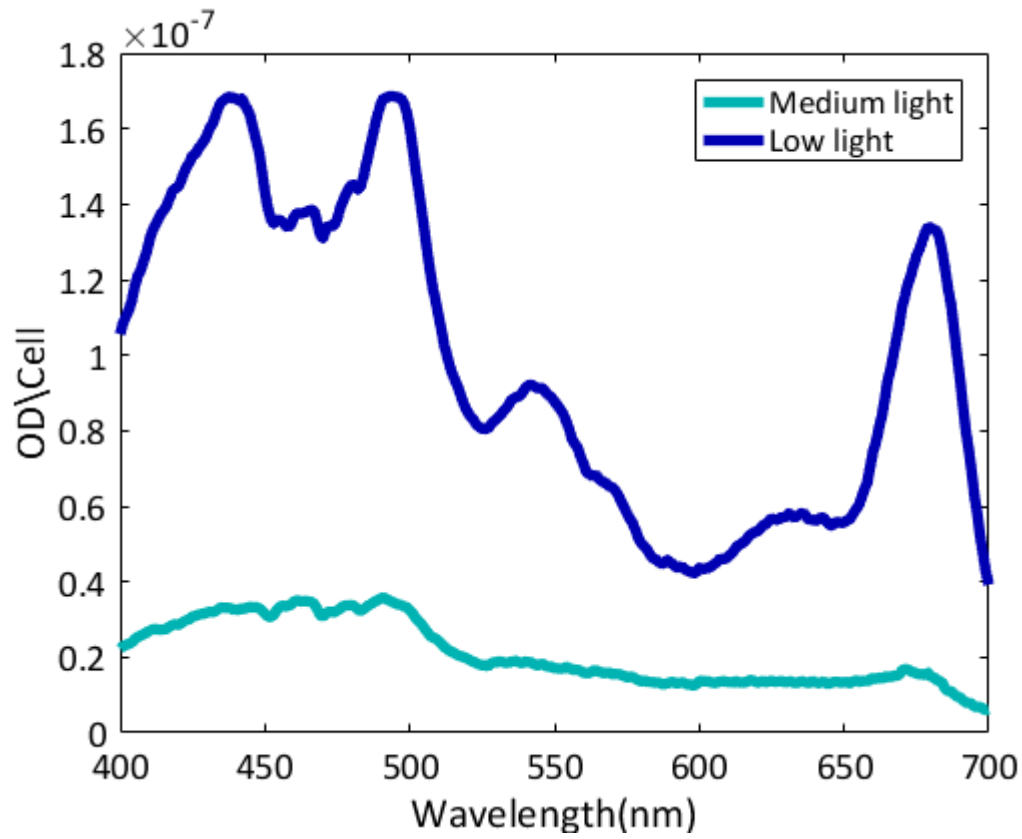


455
456

457 **Fig S5.** (A) Thylakoids preparation and photosystem complexes separation. Following 7 days
458 incubation under medium or low blue light, cells were centrifuged (12,800g for 7min) and washed
459 twice with buffer A (50mM Tris HCl pH8; 10mM NaCl; 1mM EDTA; 200mM Sorbitol). Finally,
460 cells were resuspended in 5 ml buffer A with the addition of anti-protease cocktail (Roche). Cells
461 were broken using French Press, centrifuge for 3 min using 1,160g in 4C. The supernatant was
462 collected to a new test tube and was centrifuge for 1hr using 95,000 g in 4 oC. The pellet containing
463 thylakoids, was resuspended in small volume of buffer A. Proteins concentration was determined
464 using Bradford reagents. Solubilization of membrane pigment-protein complexes was done using
465 dodecyl-maltoside (DDM 1.5 % per 1 mg protein). Thylakoids were incubated than for 30 min in ice.
466 Following incubation, thylakoids were centrifuged for 10 min using 17,000g in 4C. The supernatant
467 was loaded on sucrose gradient (0-40% in buffer A with the addition of 0.05% DDM). Gradients were
468 centrifuged 16 h at 36,000 rpm (SW41) in 4C. (B) Quantification of PsaA and PsbA in the total
469 membrane fraction by SDS-PAGE and immunoblotting. The data indicates a slightly higher PSI/PSII
470 protein content under medium light.

471

472



473

474

475 **Figure S6.** Absorption spectra of medium light and low light grown cells *in vivo*, taken prior to
476 fractionation of the cells and extraction of the pigments.

477

478

479

480